Journal of Virology

The M10 Locus of Murine Gammaherpesvirus 68 Contributes to both the Lytic and the Latent Phases of Infection

B. Flach, B. Steer, N. N. Thakur, J. Haas and H. Adler
J. Virol. **2009, 83(16):8163. DOI: 10.1128/JVI.00629-09.**
Published Ahead of Print 3 June 2009.

JOURNAL OF VIROLOGY, Aug. 2009, p. 8163–8172 Vol. 83, No. 16
0022-538X/09/$08.00+0 doi:10.1128/JVI.00629-09

The M10 Locus of Murine Gammaherpesvirus 68 Contributes to both the Lytic and the Latent Phases of Infection▽

B. Flach,[1,2] B. Steer,[1] N. N. Thakur,[1,2]§ J. Haas,[3,4] and H. Adler[1]*

Institute of Molecular Immunology, Clinical Cooperation Group Hematopoietic Cell Transplantation, Helmholtz Zentrum München—German Research Center for Environmental Health,[1] and Medical Clinic III, LMU Munich,[2] Munich, Germany; Max von Pettenkofer Institute, LMU Munich, Munich, Germany[3]; and Division of Pathway Medicine, University of Edinburgh, Edinburgh, United Kingdom[4]

Received 26 March 2009/Accepted 29 May 2009

Murine gammaherpesvirus 68 (MHV-68) is closely related to Epstein-Barr virus and Kaposi's sarcoma-associated herpesvirus (KSHV) and provides a small-animal model to study the pathogenesis of gammaherpesvirus (γHV) infections. According to the colinear organization of the γHV genomes, the M10 locus is situated at a position equivalent to the K12 locus of KSHV, which codes for proteins of the kaposin family. The M10 locus of MHV-68 has been predicted to code for three overlapping open reading frames (M10a, M10b, and M10c [M10a-c]) with unknown function. In addition, the M10 locus contains a lytic origin of replication (oriLyt). To elucidate the function of the M10 locus during lytic and latent infections, we investigated, both in vitro and in vivo, the following four recombinant viruses which were generated using MHV-68 cloned as a bacterial artificial chromosome: (i) a mutant virus with a deletion which affects both the coding region for M10a-c and the oriLyt; (ii) a revertant virus in which both the M10a-c coding region and the oriLyt were reverted to those of the wild type; (iii) a virus with an ectopic insertion of the oriLyt, which restores the function of the oriLyt but not the M10a-c coding region; and (iv) a mutant virus with a deletion in the oriLyt only. While the mutants were slightly attenuated with regard to lytic replication in cell culture, they showed severe growth defects in vivo. Both lytic replication and latency amplification were strongly reduced. In contrast, both the revertant virus and the virus with the ectopic oriLyt insertion grew very similarly to the parental wild-type virus both in vitro and in vivo. Thus, we provide genetic evidence that mutation of the oriLyt, and not of putative protein coding sequences within the M10a-c region, is responsible for the observed phenotype. We conclude that the oriLyt in the M10 locus plays an important role during infection of mice with MHV-68.

Diseases caused by gammaherpesviruses continue to be a challenge for human health. The prototypic gamma-1 herpesvirus Epstein-Barr virus (EBV) is associated with lymphomas and nasopharyngeal carcinoma (22). Human herpesvirus 8 (also called Kaposi's sarcoma-associated herpesvirus [KSHV]), a gamma-2 herpesvirus, is associated with lymphoproliferative disorders and Kaposi's sarcoma (24). In vivo studies of gammaherpesvirus pathogenesis have been limited to clinical investigation of the infection because of the restricted host range of these viruses. The murine gammaherpesvirus 68 (MHV-68) is also a member of the gammaherpesvirus subfamily and is closely related to KSHV and EBV. Since there exist no good animal models for KSHV and EBV, MHV-68 serves as a small-animal model to investigate gammaherpesvirus pathogenesis (6, 9, 10, 13, 21, 25, 26, 30). MHV-68 is a natural pathogen of wild rodents (7) and is capable of infecting laboratory mice. The nucleotide sequence of MHV-68 is similar to that of EBV and even more closely related to that of KSHV (29). MHV-68 contains genes which are homologous to cellular genes or to genes of other gammaherpesviruses. In addition, it contains virus-specific genes. Many of the latency- and transformation-associated proteins of the gammaherpesviruses, for example, EBNA and LMP of EBV, appear to be encoded by virus-specific genes, yet it has been suggested that pathogenesis-associated genes of gammaherpesviruses may be contained in similarly positioned genome regions (29). The virus-specific genes of MHV-68 were originally designated M1 to M14 (29). The M10 locus has been predicted to code for three overlapping open reading frames (M10a, M10b, and M10c [M10a-c]) (29). While several MHV-68-specific genes have been shown to code for proteins with important functions, the function of M10 is still unknown. A more recent report even considered M10a-c rather unlikely to code for proteins (21). Importantly, the M10 locus also contains a lytic origin of replication (oriLyt) (3, 8). According to the colinear organization of the gammaherpesvirus genomes, the M10 locus is situated at a position equivalent to that of the K12 locus of KSHV. K12 encodes proteins of the kaposin family. Kaposin proteins are involved in cellular transformation and in stabilization of cytokine mRNAs (16–18,20). Of note, the K12 locus also contains an oriLyt (5).

Here, we investigated the function of the M10 locus during lytic and latent infections by studying mutant viruses with deletions in the M10 loci, either affecting both the coding region for M10a-c and the oriLyt or the oriLyt only. While the mutants were slightly attenuated with regard to lytic replication in cell culture, they showed severe growth defects in vivo. Both

* Corresponding author. Mailing address: Helmholtz Zentrum München, Marchioninistr. 25, D-81377 Munich, Germany. Phone: 49-89 7099327. Fax: 49-89 7099330. E-mail: h.adler@helmholtz-muenchen.de.

§ Present address: Department of Microbiology, Sikkim University, Gangtok, India.

▽ Published ahead of print on 3 June 2009.

lytic replication and latency amplification were strongly reduced in mice infected with the mutant viruses. In contrast, a revertant virus in which both the M10a-c coding region and the oriLyt were reverted to those of the wild type and a virus with an ectopic insertion of the oriLyt which restores the function of the oriLyt but not the M10a-c coding region grew very similarly to the parental wild-type virus both in vitro and in vivo. Thus, we provide genetic evidence that mutation of the oriLyt, and not of putative protein coding sequences within the M10a-c region, is responsible for the observed phenotype.

MATERIALS AND METHODS

Cell lines. BHK-21 cells were grown in Glasgow minimal essential medium (Biochrom AG, Berlin, Germany) supplemented with 5% fetal calf serum (FCS), 5% tryptose phosphate broth, 2 mM L-glutamine, 100 U/ml penicillin, and 100 μg/ml streptomycin. Ref-Cre cells were maintained in high-glucose Dulbecco's minimal essential medium (Cell Concepts, Umkirch, Germany) supplemented with 10% FCS, 2 mM L-glutamine, 100 U/ml penicillin, 100 μg/ml streptomycin, and G418. NIH 3T3 cells were grown in high-glucose Dulbecco's minimal essential medium (Cell Concepts, Umkirch, Germany) supplemented with 10% FCS, 2 mM L-glutamine, 100 U/ml penicillin, and 100 μg/ml streptomycin.

Plasmid construction. For this study, we constructed the following four different versions of recombinant MHV-68. (i) The mutant virus ΔM10ΔTet was created by ET cloning (2, 34). For this purpose, the M10 region of MHV-68 was first replaced with a tetracycline (Tet) resistance gene flanked by FLP recombination target sites. Subsequently, the Tet resistance cassette was removed by FLP-mediated recombination, resulting in a deletion between nucleotides 99002 and 101315, which disrupts both the M10a-c coding region and the oriLyt. The procedure left a small residual insert consisting of an FLP recombination target site and short vector sequences in the disrupted region. (ii) To exclude the possibility that the observed results were due to rearrangements outside the mutated region, a revertant of the ΔM10ΔTet mutant (M10.Revertant) was generated by the two-step mutagenesis procedure (2, 19), using an unmutated 8.4-kb HindIII fragment of MHV-68 (nucleotides 95677 to 104034). (iii) We constructed a recombinant virus (OriLytΔM10ΔTet) with an ectopic insertion of the oriLyt, which restores the oriLyt but not the M10a-c coding region. For that purpose, an 863-bp SmaI-EagI fragment of MHV-68 (nucleotide positions 101139 to 102002) was cloned blunt ended into the BglII site (nucleotide position 3846 of the MHV-68 genome) of the plasmid pST76K-SR M1/M2 (12). As a result, the 863-bp fragment is flanked on both sides by homologous sequences (positions 2406 to 3846 as the 5′-end flank and positions 3847 to 6261 as the 3′-end flank) as needed for homologous recombination during the two-step mutagenesis procedure. (iv) Finally, to evaluate the impact of the oriLyt located in the M10 region, we analyzed a mutant with a deletion which renders the oriLyt nonfunctional but leaves the M10a-c coding region intact. The construction of this mutant (Δ201nt), lacking nucleotide positions 101530 to 101731, has been described previously (3). In that work, this mutant was called mutant A (Δ101530-101731).

Reconstitution and characterization of recombinant MHV-68. To reconstitute recombinant MHV-68, BHK-21 cells were transfected with 2.5 μg of bacterial artificial chromosome (BAC) MHV-68 DNA using SuperFect transfection reagent (Qiagen). When cells showed a total cytopathic effect (CPE), an aliquot of the supernatant was used to infect Ref-Cre cells carrying the Cre recombinase to remove the BAC cassette, including the green fluorescent protein sequence. BAC cassette-free viruses were identified by a limiting dilution assay on BHK-21 cells performed in a 96-well plate. All recombinant viruses were grown and titrated on BHK-21 cells, as previously described (2). Briefly, stocks were grown by infecting BHK-21 cells. After a complete CPE was shown, BHK-21 cells were harvested, and the supernatant was used as a working stock after freezing-thawing the cells two times and removing cell debris by centrifugation. Virus titers were determined by plaque assay. Briefly, 10-fold-higher dilutions were incubated on BHK-21 cells for 90 min at 37°C. After the inoculum was removed, cells were incubated for 5 days at 37°C with fresh medium containing methylcellulose. Cells were stained with crystal violet solution to determine the number of plaques.

All versions of recombinant MHV-68 were characterized by restriction enzyme analysis with different restriction enzymes and Southern blot analysis. To test in vitro growth, NIH 3T3 cells were infected at a multiplicity of infection (MOI) of 0.1 for 1 h. After the inoculum was removed, cells were incubated with fresh medium at 37°C and 5% CO_2 until the supernatants together with the cells were harvested at different time points after infection. Virus titers were determined by plaque assay, as described above.

In vivo experiments. C57BL/6 mice were purchased from Charles River Laboratories (Sulzfeld, Germany) and housed in individually ventilated cages during the MHV-68 infection period. To characterize the recombinant MHV-68 in vivo, mice were either infected intranasally (i.n.) or intraperitoneally (i.p.) with the indicated amounts of virus. Prior to i.n. infection, mice were anesthetized with ketamine and xylazine. To determine virus titers, organs were harvested at the indicated time points after infection and homogenized by Dounce homogenization or using the FastPrep-24 instrument (MP Biomedicals, Heidelberg, Germany). After freezing and thawing the homogenates two times, plaque assays were performed with 10-fold-higher dilutions of the supernatants on BHK-21 cells, as described above. For determination of the spleen weight, frequency of virus reactivation, and genomic load, spleens were harvested at the indicated time points after infection.

Limiting dilution reactivation assay. To determine the frequency of cells carrying virus reactivating from latency, threefold-higher dilutions of splenocytes (starting with 1.5×10^5 cells/well) were plated onto NIH 3T3 cells (10^4 cells/well), as described previously (1). The presence of preformed infectious virus was determined by plating parallel samples of mechanically disrupted cells (latent virus cannot reactivate from killed cells). Frequencies of reactivating cells were calculated on the basis of the Poisson distribution by determining the cell number at which 63.2% of the wells scored positive for a CPE.

Measurement of latent viral load by quantitative real-time PCR. Viral load in the spleens of infected mice was determined by quantitative real-time PCR using the ABI 7300 real-time PCR system (Applied Biosystems, Foster City, CA). DNA was extracted from spleen cells using the QIAamp DNA minikit (Qiagen, Hilden, Germany) and quantified by UV spectrophotometry. Amplification of 100 ng of DNA per reaction was performed with TaqMan universal PCR master mix under universal cycling conditions (Applied Biosystems, Foster City, CA). Using primers and probes as described previously (32), a 70-bp region of the MHV-68 glycoprotein B (gB) gene was amplified, and viral DNA copy numbers were quantified. A standard curve was created using known amounts of a plasmid containing the HindIII-N fragment of MHV-68 encompassing the gB gene. The murine ribosomal protein L8 (rpl8) was amplified in parallel and used to normalize for input DNA between samples. The primer and probe sequences for L8 were as follows: forward, 5′-CATCCCTTTGGAGGTGGTA-3′; reverse, 5′-CATCTCTTCGGATGGTGGA-3′; and probe, 5′-ACCACCAGCACATTGGCAAACC-3′. A standard curve for rpl8 was generated by a serial 10-fold-higher dilution of a plasmid containing rpl8 (RZPD clone IRAVp968B01123D6; RZPD, Berlin, Germany). The data are presented as viral genome copy numbers relative to the copy number of L8. The quantification limit was set at 50 copies per sample, according to published recommendations (28).

Statistical methods. If not otherwise indicated, data were analyzed by Student's *t* test.

RESULTS

Construction and characterization of the ΔM10ΔTet mutant and the ΔM10ΔTet revertant. To elucidate the function of the M10 locus during lytic and latent infections, we first constructed two recombinant viruses using MHV-68 cloned as a BAC (Fig. 1A, top and middle). In the ΔM10ΔTet mutant, the deletion affects both the coding region for M10a-c and the oriLyt. To prove that the phenotype of the ΔM10ΔTet mutant is due to the deletion and not due to rearrangements outside the mutated region, a revertant virus was generated by replacing the mutant fragment with a wild-type genomic fragment which reverts both the M10a-c coding region and the oriLyt to those of the wild type. The BAC-cloned genomes were analyzed by restriction enzyme analysis with several restriction enzymes and, in some cases, by sequencing the mutated region (data not shown). The genomes of the reconstituted recombinant viruses were analyzed by restriction enzyme analysis and Southern blotting (Fig. 1B).

The ΔM10ΔTet mutant shows a slight replication deficit in cell culture. To analyze the in vitro growth of the recombinant viruses, multistep growth curves were performed on NIH 3T3

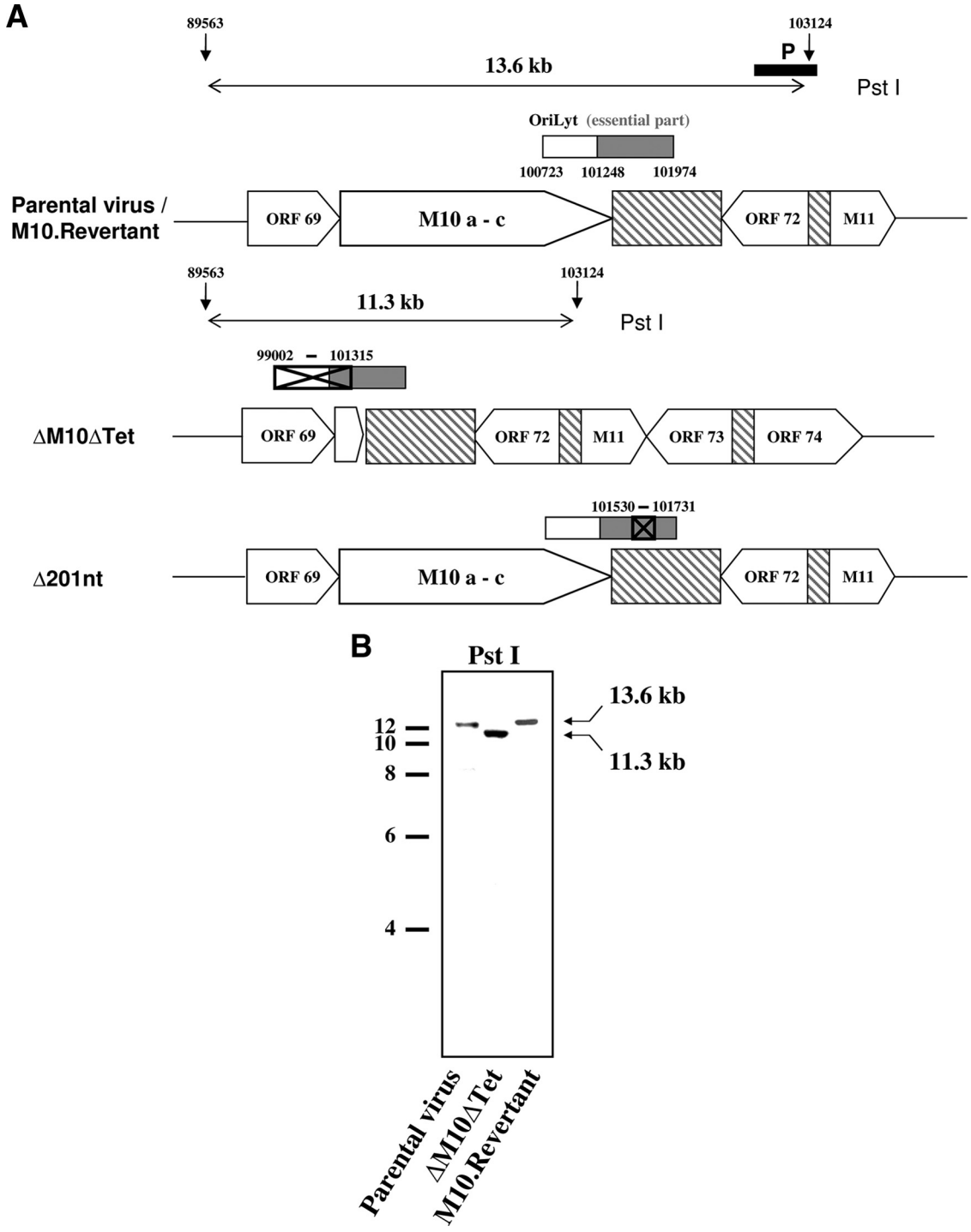

FIG. 1. Construction and characterization of the ΔM10ΔTet and Δ201nt mutants. (A) Scheme of the mutants generated. "P" indicates the probe used for Southern blot analysis, corresponding to nucleotides 102215 to 103164. The construction and characterization of the Δ201nt mutant have been described in detail previously (3). The boxed "×" schematically represents the deletion. ORF, open reading frame. (B) Southern blot analysis of viral DNA digested with the restriction enzyme PstI and hybridized with probe P. The expected fragments are indicated by arrows on the right. Marker sizes (in kilobase pairs) are indicated on the left.

cells. Compared to the parental virus, the ΔM10ΔTet mutant showed a replication deficit of approximately 1 order of magnitude. In contrast, the revertant virus attained titers similar to those of the parental virus (Fig. 2). Thus, the deletion present in the ΔM10ΔTet mutant affects lytic replication in vitro.

Reduced lytic replication in the lungs after i.n. infection with the ΔM10ΔTet mutant. To analyze lytic replication in vivo, C57BL/6 mice were i.n. infected, and viral titers were determined in lung homogenates by plaque assay. First, viral titers were determined 6 days after infection, the time point

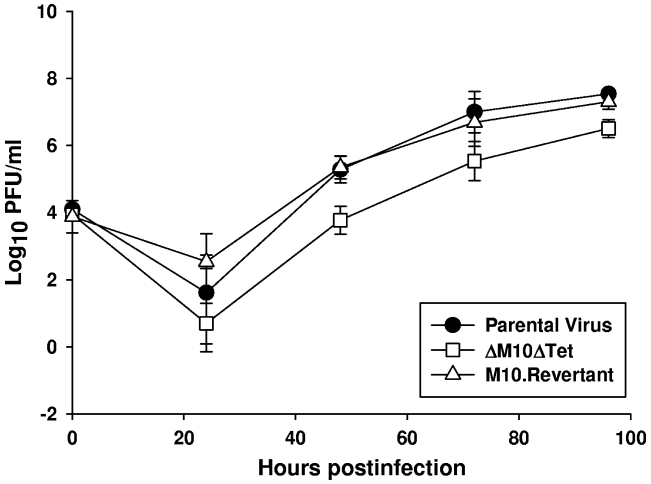

FIG. 2. Replication in cell culture. NIH 3T3 cells were infected at an MOI of 0.1 with the indicated viruses. Cells were harvested at different time points after infection, and titers were determined on BHK-21 cells. Data shown are the means ± standard deviations from three independent experiments.

when peak viral titers are usually reached. Viral titers were significantly lower after infection with the ΔM10ΔTet mutant than after infection with the parental and revertant viruses (Fig. 3A). Importantly, the viral titer in the lungs of mice infected with the M10 revertant virus was not significantly different than the viral titer in the lungs of mice infected with the parental virus, clearly indicating that the observed phenotype of the ΔM10ΔTet mutant is due to the deletion in the M10 region and not to rearrangements outside of the mutated region. Second, we compared lytic replication of the ΔM10ΔTet mutant and that of the parental virus in the lungs of mice over time after infection (Fig. 3B). At both days 3 and 6 after infection, viral titers were significantly lower after infection with the ΔM10ΔTet mutant than after infection with the parental virus. At day 10 after infection, both viruses were undetectable. We conclude from these data that the deletion present in the ΔM10ΔTet mutant affects lytic replication in the lungs of mice after i.n. infection.

The M10 region is important for latency amplification in the spleen after i.n. infection. To analyze the role of the M10 region during the latent phase of infection, C57BL/6 mice were i.n. infected, and the extent of splenomegaly, the extent of ex vivo reactivation of latently infected splenocytes, and the viral genomic load in the spleen were determined. First, we analyzed these parameters 17 days after infection, a time point around the peak of latency amplification. The spleen weight of mice infected with the ΔM10ΔTet mutant was significantly lower than the spleen weight of mice infected with the parental and revertant viruses (Fig. 4A). In addition to the spleen weight, we also determined the number of reactivating splenocytes in an ex vivo reactivation assay. Serial dilutions of live, intact splenocytes were plated on NIH 3T3 indicator cells in parallel with samples that were mechanically disrupted to distinguish between virus reactivation from latency and preformed infectious virus. No preformed infectious virus was detected for any of the viruses analyzed (data not shown). Significantly less splenocytes from mice infected with the ΔM10ΔTet mutant were reactivated compared to those infected with the parental and revertant viruses (Fig. 4B). The

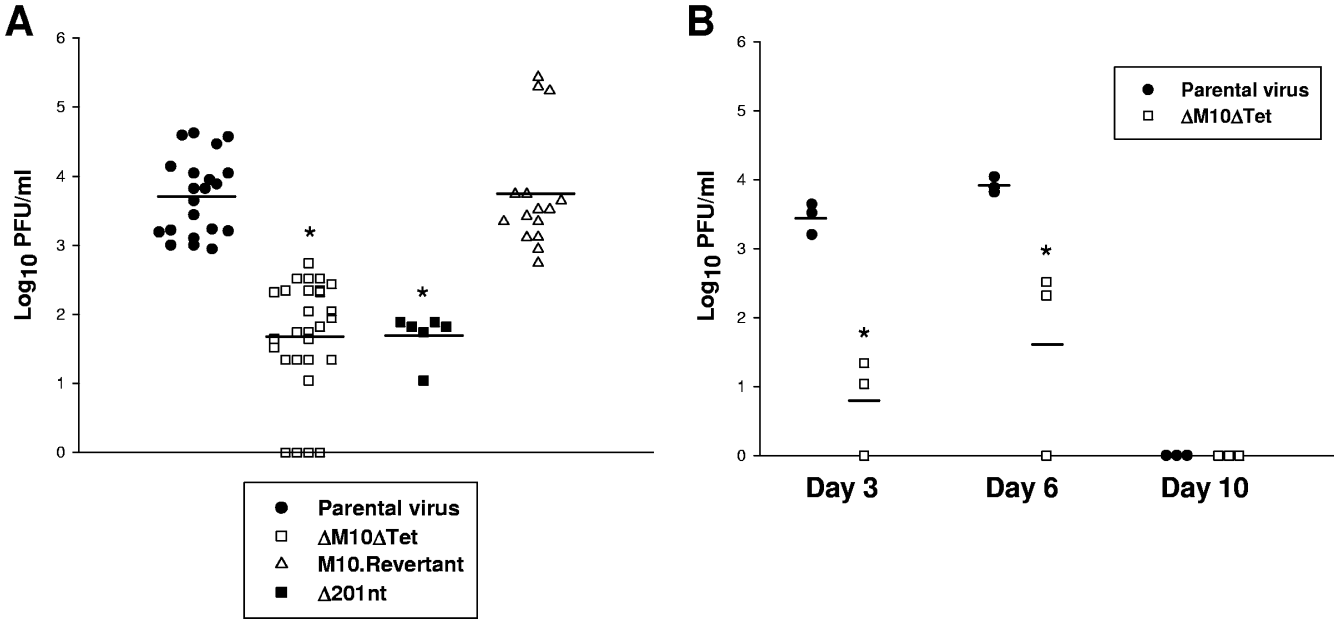

FIG. 3. Lytic replication in the lungs after i.n. infection. C57BL/6 mice were infected i.n. with 5×10^4 PFU of the indicated viruses. At day 6 after infection (A) or at the indicated time points (B), lungs were harvested, and virus titers were determined from organ homogenates by plaque assay on BHK-21 cells. Each symbol represents an individual mouse, and the bars represent the means. (A) The data are compiled from seven (parental virus), eight (ΔM10ΔTet), two (Δ201nt), and five (M10.Revertant) independent experiments; (B) the data are from a single experiment. The asterisks indicate a statistically significant difference between mutant viruses and parental and revertant viruses ($P < 0.001$) (A) and between mutant virus and parental virus ($P = 0.003$ at day 3 and $P = 0.047$ at day 6) (B).

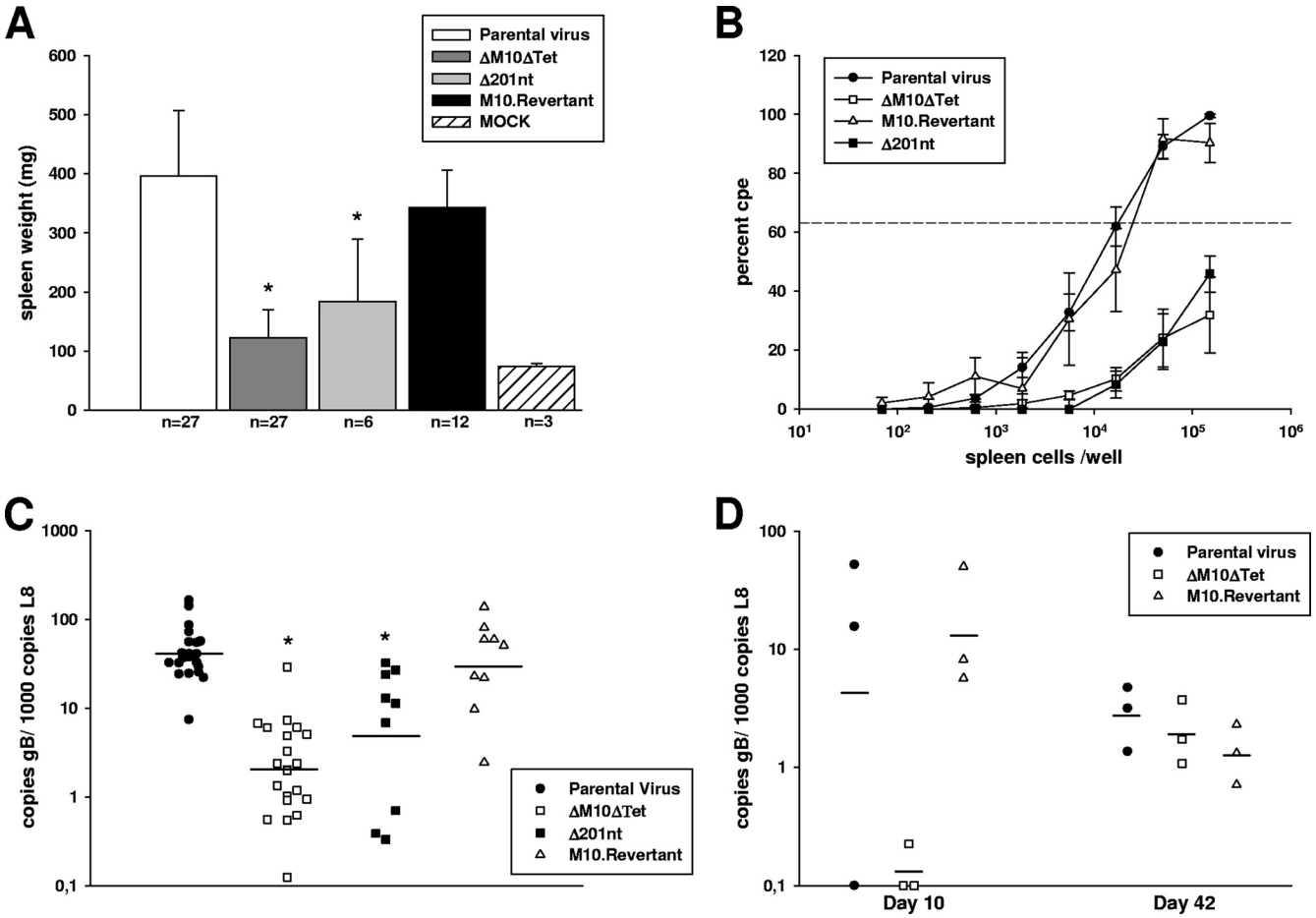

FIG. 4. Latent infection in the spleen after i.n. infection. (A) Spleen weights; (B) ex vivo reactivation of splenocytes; (C and D) viral genomic load in the spleen. C57BL/6 mice were infected i.n. with 5×10^4 PFU of the indicated viruses. At day 17 (A to C) or at days 10 and 42 after infection (D), spleens were harvested, and the spleen weights were taken. Single splenocyte suspensions were prepared and analyzed in the ex vivo reactivation assay or used for DNA isolation for real-time PCR analysis. Data shown in panel A are the means ± standard deviations of the number of individual mice indicated, compiled from nine (parental virus; ΔM10ΔTet), two (Δ201nt), and four (M10.Revertant) independent experiments. The means ± standard deviations of three uninfected mice are shown for comparison. The asterisks indicate a statistical significant difference ($P = 3.3 \times 10^{-16}$ [parental virus versus ΔM10ΔTet]; $P = 1.6 \times 10^{-5}$ [parental virus versus Δ201nt]; $P = 2.2 \times 10^{-14}$ [ΔM10ΔTet versus M10.Revertant]; and $P = 0.0003$ [Δ201nt versus M10.Revertant]). Data shown in panel B are the means ± standard errors of the means pooled from eight (parental virus), nine (ΔM10ΔTet), two (Δ201nt), and four (M10.Revertant) independent experiments. In each experiment, splenocytes from three mice per group were pooled. The dashed line in panel B indicates the point of 63.2% Poisson distribution, determined by nonlinear regression, which was used to calculate the frequency of cells reactivating lytic replication. To calculate significance, frequencies of reactivation events were statistically analyzed by paired *t* test for all cell dilutions. The statistical significance is indicated by *P* values of 0.027 (parental virus versus ΔM10ΔTet), 0.021 (parental virus versus Δ201nt), 0.022 (ΔM10ΔTet versus M10.Revertant), and 0.018 (Δ201nt versus M10.Revertant). In panels C and D, each symbol represents an individual mouse, and the bars represent the means. The data in panel C are compiled from eight (parental virus), nine (ΔM10ΔTet), three (Δ201nt), and three (M10.Revertant) independent experiments, and the data in panel D are from a single experiment. The asterisks in panel C indicate statistical significance: *P* values of 8×10^{-7} (parental virus versus ΔM10ΔTet), 0.01 (parental virus versus Δ201nt), 8×10^{-6} (ΔM10ΔTet versus M10.Revertant), and 0.024 (Δ201nt versus M10.Revertant).

frequency of reactivating splenocytes was 1 in 16.964 for the parental virus and 1 in 23.521 for the revertant virus. In contrast, the reactivation events for the ΔM10ΔTet mutant did not reach the point of 63.2% Poisson distribution and thus were too low to calculate the frequency of cells reactivating lytic replication. Using real-time PCR, we determined the genomic load in the spleens of infected mice. Consistent with the data from the ex vivo reactivation assay, the viral copy number of mice infected with the ΔM10ΔTet mutant was also significantly lower than the copy number of those infected with the parental and revertant viruses (Fig. 4C). These data indicate that the observed defect is due to a lower number of infected cells and not to a defect in reactivation. Importantly, all three parameters were not significantly different in mice infected with the M10 revertant virus when compared to the parental virus, again clearly indicating that the observed phenotype of the ΔM10ΔTet mutant is due to the deletion in the M10 region and not to rearrangements outside of the mutated region. Additionally, we compared the genomic load in the spleens of infected mice at two additional time points. At day 10 after infection, a time point when latency establishment takes place, the genomic load in mice infected with the ΔM10ΔTet mutant was considerably lower than that in mice infected with either parental virus or revertant virus (Fig. 4D). However, the difference did not

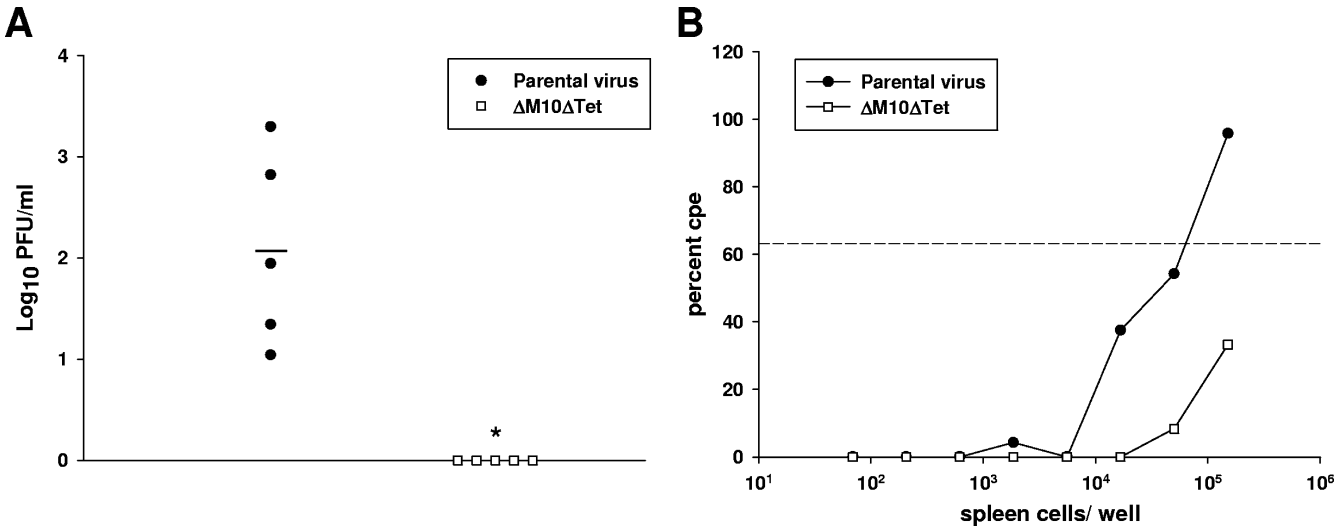

FIG. 5. Lytic replication and latent infection in the spleen after i.p. infection. C57BL/6 mice were infected i.p. with 1×10^5 PFU of the indicated viruses. (A) Spleen titer. At day 6 after infection, spleens were harvested, and virus titers were determined from organ homogenates by plaque assay on BHK-21 cells. Each symbol represents an individual mouse, and the bar represents the mean. The data were compiled from two independent experiments. The asterisk indicates a statistically significant difference ($P = 0.001$). (B) Ex vivo reactivation of splenocytes. At day 17 after infection, spleens were harvested, and single splenocyte suspensions were prepared and analyzed in the ex vivo reactivation assay. Data shown are the means from a single experiment, with pooled splenocytes from three mice per group. The dashed line indicates the point of 63.2% Poisson distribution, determined by nonlinear regression, which was used to calculate the frequency of cells reactivating lytic replication. To calculate significance, frequencies of reactivation events were statistically analyzed by paired *t* test for all cell dilutions. The statistical significance of the difference between the mutant and parental viruses is a *P* value of 0.07.

reach statistical significance due to the small number of mice tested and the variability between individual mice. At day 42 after infection, the genomic loads were comparable in all groups of mice. Thus, taking all three independent measurements of viral latency together, we conclude that the deletion present in the ΔM10ΔTet mutant does also influence latency after i.n. infection.

Lytic replication and latency in the spleen are also reduced after i.p. infection with the ΔM10ΔTet mutant. Since it has been described that the phenotype of MHV-68 mutants may depend on the route used for infection (15), we also analyzed the phenotype of the ΔM10ΔTet mutant after i.p. infection. For this purpose, mice were infected i.p. with 1×10^5 PFU of either parental virus or the ΔM10ΔTet mutant. First, spleens were harvested 6 days after infection, and lytic virus titers were determined from organ homogenates by plaque assay. Lytic virus was detected in all mice after infection with the parental virus. However, no virus was detected after infection with the ΔM10ΔTet mutant (Fig. 5A). It should be noted that after i.p. infection, the peak of acute infection in the spleen is around day 9 after infection (31). Thus, it is likely that at a later time point, lytic virus would also be detectable in mice infected i.p. with the ΔM10ΔTet mutant. Nevertheless, the data clearly indicate that the deletion present in the ΔM10ΔTet mutant also affects lytic replication after i.p. infection. Second, spleens were harvested 17 days after infection and analyzed by the ex vivo reactivation assay (Fig. 5B). As after i.n. infection, less splenocytes reactivated from mice infected with the ΔM10ΔTet mutant than from mice infected with the parental virus. The frequency of reactivating splenocytes was 1 in 57.094 for the parental virus. In contrast, the reactivation events for the ΔM10ΔTet mutant did not reach the point of the 63.2% Poisson distribution and thus were too low to calculate the frequency of cells reactivating lytic replication. No preformed infectious virus was detected for any of the viruses analyzed (data not shown). The data shown in Fig. 5B are from a single experiment only (with pooled splenocytes from three mice per group). However, the experiment was repeated twice with two additional infection doses (1×10^6 and 1×10^4 PFU), which yielded comparable results (data not shown). Thus, the deletion present in the ΔM10ΔTet mutant also influences latency after i.p. infection.

Ectopic complementation of the oriLyt restores the phenotype of the ΔM10ΔTet mutant. Since (i) others considered M10a-c unlikely to code for proteins (21) and (ii) we were not able to detect M10 proteins (data not shown; see Discussion), we hypothesized that the observed phenotype of the ΔM10ΔTet mutant might be due to the mutation in the oriLyt. As described above, in the ΔM10ΔTet mutant, both the coding region for M10a-c and the oriLyt are mutated. Thus, a virus with a mutated M10 region but an intact oriLyt should behave like the parental virus if the observed phenotype is due to mutation of the oriLyt and not the putative protein coding sequences within the M10a-c region. To test this hypothesis, we ectopically inserted an 863-bp fragment, containing the entire essential region of the oriLyt, into the ΔM10ΔTet mutant, thereby restoring the function of the oriLyt but not the M10a-c coding region in the resulting virus OriLytΔM10ΔTet (Fig. 6A and B).

First, we analyzed the in vitro growth of the OriLytΔM10ΔTet virus. For this purpose, multistep growth curves were generated from NIH 3T3 cells. As shown before, the ΔM10ΔTet mutant showed a replication deficit of approximately 1 order of magnitude compared to that of the parental virus. In contrast, the OriLytΔM10ΔTet virus attained titers similar to those of the

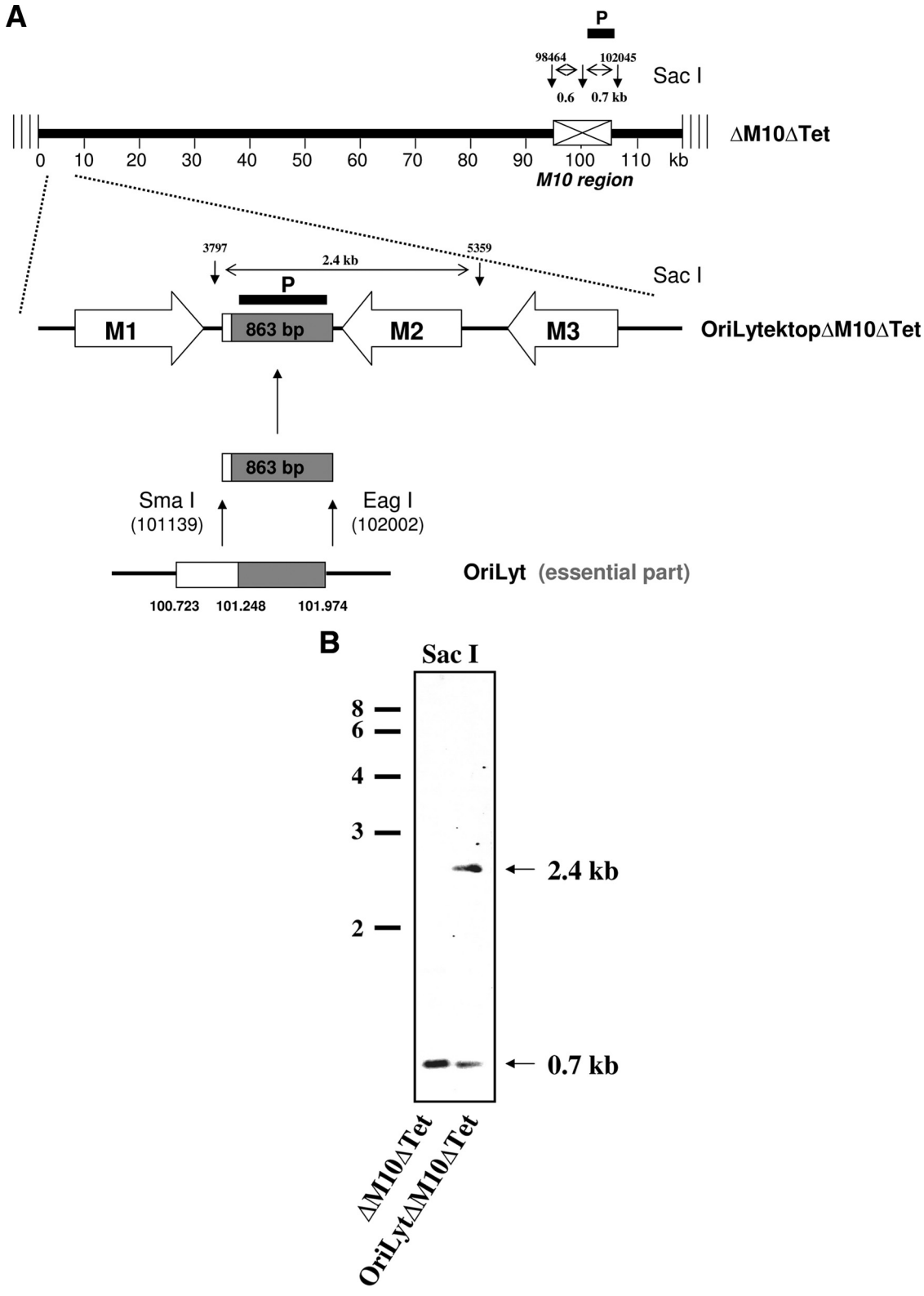

FIG. 6. Construction and characterization of the OriLytΔM10ΔTet mutant. (A) Schematic map of the OriLytΔM10ΔTet mutant genome, with the ectopic insertion of the essential part of the oriLyt indicated. P, probe. (B) Southern blot analysis of viral DNA digested with the restriction enzyme SacI and hybridized with the 863-bp SmaI-EagI fragment, indicated in panel A as the probe. The expected fragments are indicated by arrows on the right. Marker sizes (in kilobase pairs) are indicated on the left.

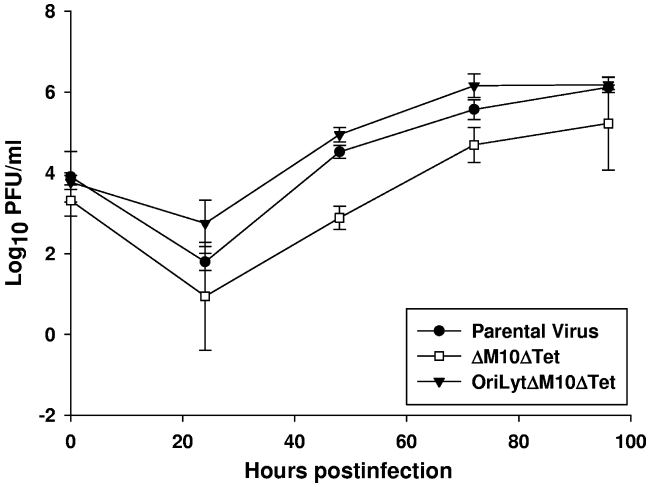

FIG. 7. Replication in cell culture. NIH 3T3 cells were infected at an MOI of 0.1 with the indicated viruses. Cells were harvested at different time points after infection, and titers were determined on BHK-21 cells. Data shown are the means ± standard deviations from two independent experiments.

parental virus (Fig. 7). Thus, ectopic insertion of the oriLyt completely restores the in vitro phenotype of the ΔM10ΔTet mutant.

Next, we analyzed lytic replication in vivo. C57BL/6 mice were i.n. infected, and viral titers were determined in lung homogenates by plaque assay 6 days after infection. Consistent with the previous results, the ΔM10ΔTet mutant showed a significant replication deficit. However, ectopic insertion of the oriLyt completely restored the phenotype of the ΔM10ΔTet mutant (Fig. 8A). Finally, we analyzed the latent phase after infection with the OriLytΔM10ΔTet virus. C57BL/6 mice were i.n. infected, and the extent of splenomegaly, the extent of ex vivo reactivation of latently infected splenocytes, and the viral genomic load in the spleen were determined 17 days after infection. There was no significant difference in the spleen weight (Fig. 8B), in the frequency of ex vivo reactivation (1 in 10.510 and 1 in 4.176) (Fig. 8C), and in the viral genomic load (Fig. 8D) between parental virus and the OriLytΔM10ΔTet virus, respectively, while the ΔM10ΔTet mutant showed reduced fitness for all parameters. Thus, ectopic insertion of the oriLyt completely restored the phenotype of the ΔM10ΔTet mutant for all three latency parameters.

A mutant with a deletion which affects the oriLyt exclusively, but leaves the M10a-c coding sequences intact (Δ201nt mutant), shows the same phenotype as the ΔM10ΔTet mutant. The result that ectopic insertion of the oriLyt in the ΔM10ΔTet mutant completely restored the phenotype already suggested that the observed phenotype of the ΔM10ΔTet mutant is due to mutation of the oriLyt and not of putative protein coding sequences within the M10a-c region. To further confirm this, we analyzed a mutant with a deletion which renders the oriLyt nonfunctional but leaves the M10a-c coding region intact. The construction and characterization of this mutant, lacking nucleotide positions 101530 to 101731 (Δ201nt) (schematically shown in Fig. 1A, bottom), have been described in detail previously (3). In the previous work, we had also demonstrated that the Δ201nt mutant displays a slight replication deficit in cell culture, just as the ΔM10ΔTet mutant does. However, the in vivo phenotype had not been investigated yet. Therefore, we analyzed here the in vivo phenotype of the Δ201nt mutant and compared it to the phenotype of the ΔM10ΔTet mutant. The Δ201nt mutant showed a reduction in lytic replication in the lung after i.n. infection to exactly the same extent as the ΔM10ΔTet mutant did (Fig. 3A). In addition, all latency parameters measured (spleen weight, ex vivo reactivation of latently infected splenocytes, and viral genomic load in the spleen) were equally reduced after infection with the Δ201nt mutant, as they were after infection with the ΔM10ΔTet mutant (Fig. 4A to C). These data do further support our conclusion that the phenotype caused by mutation of the M10 locus is due to mutation of the oriLyt and not due to mutation of putative protein coding sequences within the M10a-c region.

DISCUSSION

While the function of several MHV-68-specific genes has been elucidated, the function of M10a-c has not been investigated so far. The M10 locus has initially been predicted to include three overlapping open reading frames (M10a-c) (29). In addition, the M10 locus contains an oriLyt (8) and a repetitive region termed the 100-bp repeat region. The latter region has recently been described as a ligand for the induction of type I interferon (23). In this study, we investigated the function of the M10 locus during lytic and latent infections of mice with MHV-68 by analyzing mutant viruses with deletions in the M10 locus, either affecting both the predicted coding region for M10a-c and the oriLyt or the oriLyt only. While the mutants were slightly attenuated with regard to lytic replication in cell culture, they showed severe growth defects in vivo. Both lytic replication and latency amplification were strongly reduced in mice infected with the mutant viruses. In contrast, a revertant virus in which both the M10a-c coding region and the oriLyt were reverted to those of the wild type and a virus with an ectopic insertion of the oriLyt which restores the function of the oriLyt but not the M10a-c coding region grew very similarly to the parental wild-type virus both in vitro and in vivo. Thus, we propose that mutation of the oriLyt, and not mutation of putative protein coding sequences within the M10a-c region, is responsible for the observed phenotype. This is also consistent with our failure to demonstrate expression of a protein(s) from the M10 region (data not shown). Although a recent report considered M10a-c unlikely to code for proteins (21), we nonetheless undertook two different approaches to detect potential proteins encoded by the M10 region, as follows: (i) two polyclonal rabbit antisera were raised against two synthetic peptides (GNRGDGAPERGSG and PGARERAARPGVR) from the M10 region, and (ii) a recombinant MHV-68, in which the product of the M10a open reading frame was C-terminally tagged by a hemagglutinin (HA) tag, was constructed. With the polyclonal rabbit antisera, Western blots were performed with lysates or supernatants from lytically infected NIH 3T3 cells at various times after infection and also from the latently infected cell line S11 (27), with the latter cells either left untreated or treated with tetradecanoyl phorbol acetate to induce the lytic cycle. To detect a potential HA-tagged M10a protein, NIH 3T3 cells were infected with the recombinant MHV-68-M10aHA-tag, and Western blots (with or without preceding immunoprecipitation) were performed

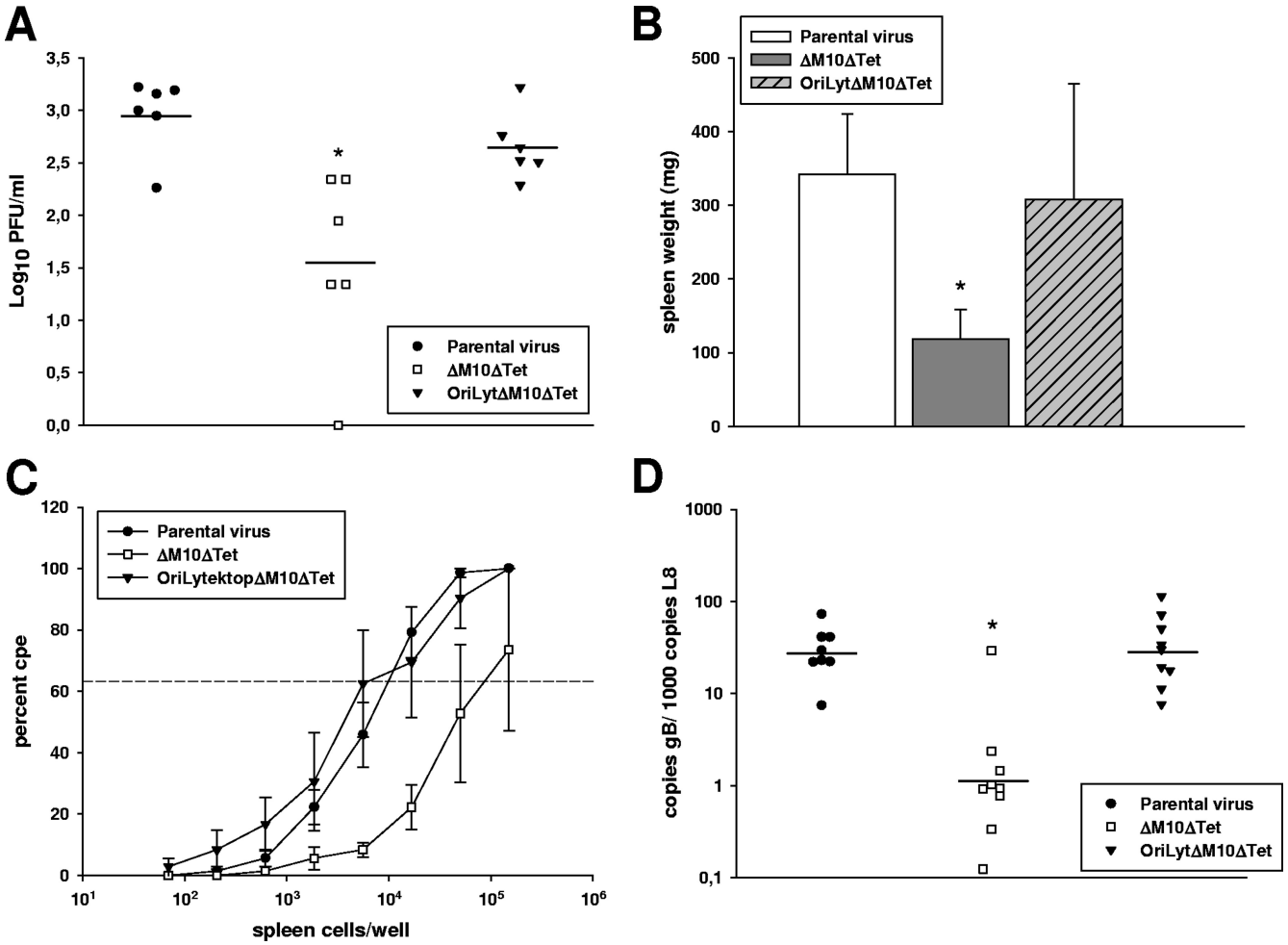

FIG. 8. Ectopic complementation of the oriLyt restores the phenotype of the ΔM10ΔTet mutant. C57BL/6 mice were infected i.n. with 5×10^4 PFU of the indicated viruses. (A) Lytic lung titer. At day 6 after infection, lungs were harvested, and virus titers were determined from organ homogenates by plaque assay on BHK-21 cells. Each symbol represents an individual mouse, and the bars represent the means. The data are compiled from two independent experiments. The asterisk indicates a statistically significant difference ($P = 0.004$ [parental virus versus ΔM10ΔTet] and $P = 0.016$ [ΔM10ΔTet versus OriLytΔM10ΔTet]). (B) Splenomegaly; (C) ex vivo reactivation of splenocytes; (D) viral genomic load in the spleen. At day 17 after infection, spleens were harvested, and the spleen weights were taken. Single splenocyte suspensions were prepared and analyzed in the ex vivo reactivation assay or used for DNA isolation for real-time PCR analysis. Data shown in panel B are the means ± standard deviations of nine mice per group, compiled from three independent experiments. The asterisk indicates a statistically significant difference ($P = 2.5 \times 10^{-6}$ [parental virus versus ΔM10ΔTet] and $P = 0.0029$ [ΔM10ΔTet versus OriLytΔM10ΔTet]). Data shown in panel C are the means ± standard errors of the means pooled from three independent experiments. In each experiment, splenocytes from three mice per group were pooled. Serial dilutions of live, intact splenocytes were plated on NIH 3T3 indicator cells in parallel with samples that were mechanically disrupted to distinguish between virus reactivation from latency and preformed infectious virus. No preformed infectious virus was detected with any of the viruses analyzed (data not shown). The dashed line in panel C indicates the point of 63.2% Poisson distribution, determined by nonlinear regression, which was used to calculate the frequency of cells reactivating lytic replication. To calculate significance, frequencies of reactivation events were statistically analyzed by paired *t* test for all cell dilutions. The statistical significance is indicated by *P* values of 0.0177 (parental virus versus ΔM10ΔTet) and 0.004 (ΔM10ΔTet versus OriLytΔM10Δtet). In panel D, each symbol represents an individual mouse, and the bars represent the means. The data are compiled from three independent experiments. The asterisk indicates a statistically significant difference ($P = 0.001$ [parental virus versus ΔM10ΔTet] and $P = 0.008$ [ΔM10ΔTet versus OriLytΔM10ΔTet]).

with lysates or supernatants from various times after infection. Neither with the peptide-specific sera nor with a HA-specific antibody could expression of M10 proteins be detected (data not shown). Clearly, we cannot formally exclude protein expression; however, the data are in accordance with a report which considered M10a-c rather unlikely to code for proteins (21). While protein expression has never been demonstrated from the M10 locus, expression of mRNAs was shown by others by microarray and/or reverse transcription-PCR assays (4, 11).

In contrast to our observations, it has recently been reported that MHV-68 BACs with mutations in or close to the 100-bp region are unable to produce progeny virions (23). Specifically, transfection of cells with BACs with transposon insertions at nucleotide positions 100952 or 101278 did not lead to virus production. In contrast to our mutants, those mutants were

generated by transposon mutagenesis, which does not lead to the deletion of viral sequences but to an additional insertion of a 1.3-kb transposon sequence. Importantly, construction of revertant viruses was not reported. Thus, it is possible that the presence of the large transposon insertion and/or unwanted changes elsewhere in the genome which might have occurred during the mutagenesis procedure are responsible for the observed differences. In our hands, infectious virus from two different BAC mutants with deletions in the M10 region could be reconstituted, and both mutants showed comparable phenotypes. In addition, the generation of a revertant virus clearly demonstrated that the observed phenotype of the corresponding mutant is due to the deletion in the M10 region and not to rearrangements outside of the mutated region.

Consistent with our previous findings (3), the mutants were slightly attenuated only with regard to lytic replication in cell culture. Obviously, the remaining second oriLyt is sufficient for efficient lytic replication in fibroblasts in vitro. In contrast, in vivo, lytic replication was strongly reduced in mice infected with the mutant viruses, suggesting that the oriLyt requirements for lytic replication may be different in vitro and in vivo. Of note, latency amplification was also affected. We hypothesize that virus reactivation, subsequent lytic replication, and reinfection contribute to the amplification of latency. Consistent with this hypothesis is the suggestion by others that ongoing productive replication and virus reactivation may reseed latency reservoirs, thereby increasing the level of latently infected cells (14, 33).

Taking these results together, we conclude that the M10 locus plays an important role during infection of mice with MHV-68 and that mutation of the oriLyt but not mutation of putative protein coding sequences within the M10 region critically affects both lytic and latent infections in vivo.

ACKNOWLEDGMENTS

This work was supported by grants from the Deutsche Forschungsgemeinschaft (Ad121/2-1 to -2-4) and the BMBF (NGFN-Plus, FKZ 01GS0802) to H.A.

We are grateful to K. Freimüller and to the members of our animal facilities for expert technical assistance. We also thank B. Adler for critically reading the manuscript.

REFERENCES

1. **Adler, H., M. Messerle, and U. H. Koszinowski.** 2001. Virus reconstituted from infectious bacterial artificial chromosome (BAC)-cloned murine gammaherpesvirus 68 acquires wild-type properties in vivo only after excision of BAC vector sequences. J. Virol. **75:**5692–5696.
2. **Adler, H., M. Messerle, M. Wagner, and U. H. Koszinowski.** 2000. Cloning and mutagenesis of the murine gammaherpesvirus 68 genome as an infectious bacterial artificial chromosome. J. Virol. **74:**6964–6974.
3. **Adler, H., B. Steer, K. Freimuller, and J. Haas.** 2007. Murine gammaherpesvirus 68 contains two functional lytic origins of replication. J. Virol. **81:**7300–7305.
4. **Ahn, J. W., K. L. Powell, P. Kellam, and D. G. Alber.** 2002. Gammaherpesvirus lytic gene expression as characterized by DNA array. J. Virol. **76:**6244–6256.
5. **AuCoin, D. P., K. S. Colletti, Y. Xu, S. A. Cei, and G. S. Pari.** 2002. Kaposi's sarcoma-associated herpesvirus (human herpesvirus 8) contains two functional lytic origins of DNA replication. J. Virol. **76:**7890–7896.
6. **Blackman, M. A., and E. Flano.** 2002. Persistent γ-herpesvirus infections: what can we learn from an experimental mouse model? J. Exp. Med. **195:** F29–F32.
7. **Blaskovic, D., M. Stancekova, J. Svobodova, and J. Mistrikova.** 1980. Isolation of five strains of herpesviruses from two species of free living small rodents. Acta Virol. **24:**468.
8. **Deng, H., J. T. Chu, N. H. Park, and R. Sun.** 2004. Identification of *cis* sequences required for lytic DNA replication and packaging of murine gammaherpesvirus 68. J. Virol. **78:**9123–9131.
9. **Doherty, P. C., J. P. Christensen, G. T. Belz, P. G. Stevenson, and M. Y. Sangster.** 2001. Dissecting the host response to a gamma-herpesvirus. Philos. Trans. R. Soc. Lond. B **356:**581–593.
10. **Doherty, P. C., R. A. Tripp, A.-M. Hamilton-Easton, R. D. Cardin, D. L. Woodland, and M. A. Blackman.** 1997. Tuning into immunological dissonance: an experimental model for infectious mononucleosis. Curr. Opin. Immunol. **9:**477–483.
11. **Ebrahimi, B., B. M. Dutia, K. L. Roberts, J. J. Garcia-Ramirez, P. Dickinson, J. P. Stewart, P. Ghazal, D. J. Roy, and A. A. Nash.** 2003. Transcriptome profile of murine gammaherpesvirus-68 lytic infection. J. Gen. Virol. **84:**99–109.
12. **El-Gogo, S., C. Staib, J. J. Lasarte, G. Sutter, and H. Adler.** 2007. Recombinant murine gammaherpesvirus 68 (MHV-68) as challenge virus to test efficacy of vaccination against chronic virus infections in the mouse model. Vaccine **25:**3934–3945.
13. **Flano, E., D. L. Woodland, and M. A. Blackman.** 2002. A mouse model for infectious mononucleosis. Immunol. Res. **25:**201–217.
14. **Gangappa, S., S. B. Kapadia, S. H. Speck, and H. W. Virgin IV.** 2002. Antibody to a lytic cycle viral protein decreases gammaherpesvirus latency in B-cell-deficient mice. J. Virol. **76:**11460–11468.
15. **Jacoby, M. A., H. W. Virgin IV, and S. H. Speck.** 2002. Disruption of the M2 gene of murine gammaherpesvirus 68 alters splenic latency following intranasal, but not intraperitoneal, inoculation. J. Virol. **76:**1790–1801.
16. **Kliche, S., W. Nagel, E. Kremmer, C. Atzler, A. Ege, T. Knorr, U. Koszinowski, W. Kolanus, and J. Haas.** 2001. Signaling by human herpesvirus 8 kaposin A through direct membrane recruitment of cytohesin-1. Mol. Cell **7:**833–843.
17. **McCormick, C., and D. Ganem.** 2005. The kaposin B protein of KSHV activates the p38/MK2 pathway and stabilizes cytokine mRNAs. Science **307:**739–741.
18. **McCormick, C., and D. Ganem.** 2006. Phosphorylation and function of the kaposin B direct repeats of Kaposi's sarcoma-associated herpesvirus. J. Virol. **80:**6165–6170.
19. **Messerle, M., I. Crnkovic, W. Hammerschmidt, H. Ziegler, and U. H. Koszinowski.** 1997. Cloning and mutagenesis of a herpesvirus genome as an infectious bacterial artificial chromosome. Proc. Natl. Acad. Sci. USA **94:** 14759–14763.
20. **Muralidhar, S., A. M. Pumfery, M. Hassani, M. R. Sadaie, N. Azumi, M. Kishishita, J. N. Brady, J. Doniger, P. Medveczky, and L. J. Rosenthal.** 1998. Identification of kaposin (open reading frame K12) as a human herpesvirus 8 (Kaposi's sarcoma-associated herpesvirus) transforming gene. J. Virol. **72:**4980–4988.
21. **Nash, A. A., B. M. Dutia, J. P. Stewart, and A. J. Davison.** 2001. Natural history of murine γ-herpesvirus infection. Philos. Trans. R. Soc. Lond. B **356:**569–579.
22. **Rickinson, A. B., and E. Kieff.** 2001. Epstein-Barr virus, p. 2575–2627. *In* D. M. Knipe, P. M. Howley, D. E. Griffin, M. A. Martin, R. A. Lamb, B. Roizman, and S. E. Straus (ed.), Fields virology, 4th ed. Lippincott Williams & Wilkins, Philadelphia, PA.
23. **Sanchez, D. J., D. Miranda, Jr., V. Arumugaswami, S. Hwang, A. E. Singer, A. Senaati, A. Shahangian, M. J. Song, R. Sun, and G. Cheng.** 2008. A repetitive region of gammaherpesvirus genomic DNA is a ligand for induction of type I interferon. J. Virol. **82:**2208–2217.
24. **Schulz, T. F.** 1998. Kaposi's sarcoma-associated herpesvirus (human herpesvirus-8). J. Gen. Virol. **79:**1573–1591.
25. **Simas, J. P., and S. Efstathiou.** 1998. Murine gammaherpesvirus 68: a model for the study of gammaherpesvirus pathogenesis. Trends Microbiol. **6:**276–282.
26. **Speck, S. H., and H. W. Virgin IV.** 1999. Host and viral genetics of chronic infection: a mouse model of gamma-herpesvirus pathogenesis. Curr. Opin. Microbiol. **2:**403–409.
27. **Usherwood, E. J., J. P. Stewart, and A. A. Nash.** 1996. Characterization of tumor cell lines derived from murine gammaherpesvirus-68-infected mice. J. Virol. **70:**6516–6518.
28. **Vaerman, J. L., P. Saussoy, and I. Ingargiola.** 2004. Evaluation of real-time PCR data. J. Biol. Regul. Homeost. Agents **18:**212–214.
29. **Virgin, H. W., IV, P. Latreille, P. Wamsley, K. Hallsworth, K. E. Weck, A. J. Dal Canto, and S. H. Speck.** 1997. Complete sequence and genomic analysis of murine gammaherpesvirus 68. J. Virol. **71:**5894–5904.
30. **Virgin, H. W., IV, and S. H. Speck.** 1999. Unraveling immunity to γ-herpesviruses: a new model for understanding the role of immunity in chronic virus infection. Curr. Opin. Immunol. **11:**371–379.
31. **Weck, K. E., M. L. Barkon, L. I. Yoo, S. H. Speck, and H. W. Virgin IV.** 1996. Mature B cells are required for acute splenic infection, but not for establishment of latency, by murine gammaherpesvirus 68. J. Virol. **70:**6775–6780.
32. **Weinberg, J. B., M. L. Lutzke, R. Alfinito, and R. Rochford.** 2004. Mouse strain differences in the chemokine response to acute lung infection with a murine gammaherpesvirus. Viral Immunol. **17:**69–77.
33. **Willer, D. O., and S. H. Speck.** 2005. Establishment and maintenance of long-term murine gammaherpesvirus 68 latency in B cells in the absence of CD40. J. Virol. **79:**2891–2899.
34. **Zhang, Y., J. P. Muyrers, G. Testa, and A. F. Stewart.** 2000. DNA cloning by homologous recombination in Escherichia coli. Nat. Biotechnol. **18:**1314–1317.